PNAS RESEARCH ARTICLE | PHYSIOLOGY

High energetic cost of color change in octopuses

Sofie C. Sonner[a] and Kirt L. Onthank[a,1]

Edited by John Speakman, Chinese Academy of Sciences, Shenzhen, United Kingdom; received April 26, 2024; accepted October 11, 2024

For many animals, color change is a critical adaptive mechanism believed to carry a substantial energetic cost. Yet, no study to date has directly measured the energy expenditure associated with this process. We examined the metabolic cost of color change in octopuses by measuring oxygen consumption in samples of excised octopus skin during periods of chromatophore expansion and contraction and then modeled metabolic demand over the whole octopus as a function of octopus mass. The metabolic demand of the fully activated chromatophore system is nearly as great as an octopus's resting metabolic rate. This high metabolic cost carries ecological and evolutionary implications, including selective pressures in octopuses that may influence the adoption of nocturnal lifestyles, the use of dens, the reduction of the chromatophore system in deep-sea species, and metabolic trade-offs associated with foraging.

metabolism | camouflage | chromatophores | physiological cost | phenotypic plasticity

Significance

Rapid color change is an adaptation that has evolved multiple times in animals and is used for dynamic camouflage, communication, thermoregulation, or ultraviolet light protection. However, understanding the evolution of this phenomenon is hindered by a lack of information on the costs associated with rapid color change. Using octopuses as a model, a group whose members have one of the most advanced color change systems in the animal kingdom, our study found that rapid color change is exceptionally energetically expensive, nearly as great as the organism's resting metabolic rate.

The phenomenon of rapid color change, occurring within milliseconds to hours, has evolved independently multiple times across a diverse array of animal taxa including in amphibians, reptiles, fish, arthropods, and mollusks, showcasing its widespread adaptive significance. The ability to change color is used by animals for a variety of purposes, including camouflage, communication, thermoregulation, or ultraviolet light protection (1). Understanding the evolution of this striking example of phenotypic plasticity requires a detailed understanding of the costs and benefits of this trait. While there is extensive evidence of the multiple benefits afforded by the ability to change color, there exists virtually no information on the costs associated with this trait.

Color change can either be caused relatively slowly by the production or destruction of pigments, known as morphological color change, or occur more rapidly by the relocation of existing pigments within the skin, known as physiological color change (2). It is widely assumed that color change in animals carries a metabolic cost due to the energy required for pigment production, catabolism, and physical relocation; resource allocation; and environmental monitoring (2–4). To understand the evolution of color change in animals, a robust understanding of the metabolic costs associated with color change mechanisms is needed; however, to date, few studies have attempted to measure these costs (2). Only two studies have examined the energetic cost of color change. Both induced color change by placing organisms into light or dark background enclosures, one using food consumption as a proxy for energy usage (2–4) and the other performing respirometry to measure the metabolic rate of organisms after color change (5). However, this experimental approach does not directly measure the mechanism of color change and is vulnerable to the possibility that the observed changes in energetics could have been a result of stress induced in the organisms by the color of their environment and not directly due to the process of color change itself. These studies illustrate the extreme difficulty of isolating the mechanism of color change when attempting to measure the energetic costs of this process. Despite the challenges in quantifying the energetic cost of color change, it remains crucial to study such phenomena in organisms in which color change plays a pivotal role in their biology, such as cephalopods.

Cephalopod color change, in regard to speed of change and diversity of patterns, is unparalleled among other animals (6). This involves a variety of mechanisms, most important of which are the chromatophore organs in the skin-pigment sacs each with 15 to 25 radial muscle fibers innervated by neurons (3, 7). When these muscles contract, the pigment sac expands from a spherical shape approximately 10 μm in diameter to a flattened disk approximately 300 μm in diameter, thereby providing coloration to a small portion of the skin (8, 9). With approximately 230 chromatophores per square millimeter of skin in octopuses, the chromatophore system enables a wide array of complex skin coloration patterns (8). Due to the involvement of the nervous and muscular systems, it is likely that cephalopod color change is one of the most metabolically expensive forms of animal color change. We set out to determine the metabolic cost of chromatophore use in octopuses by measuring the difference in oxygen consumption of excised skin between periods of

Author affiliations: [a]Department of Biological Sciences, Walla Walla University, College Place, WA 99324

Author contributions: S.C.S. and K.L.O. designed research; performed research; contributed new reagents/analytic tools; analyzed data; and wrote the paper.

The authors declare no competing interest.

This article is a PNAS Direct Submission.

[1]To whom correspondence may be addressed. Email: kirt.onthank@wallawalla.edu.

This article contains supporting information online at https://www.pnas.org/lookup/suppl/doi:10.1073/pnas.2408386121/-/DCSupplemental.

Published November 18, 2024.

chromatophore expansion and contraction. In octopuses, chromatophores in excised skin have been shown to expand when exposed to bright light, a behavior called light-activated chromatophore expansion, or LACE (10). This unique phenomenon allows for the manipulation of octopus chromatophore function, enabling experimental approaches not possible in other color change systems. In this study, we estimate the metabolic demand of the octopus chromatophore system.

Results

Metabolic Rate Determination of Excised Skin. To estimate the metabolic rate of chromatophores, we measured oxygen consumption ($\dot{V}O_2$), a commonly used proxy for metabolic rate, of 17 samples of excised skin of *Octopus rubescens*, with chromatophores expanded by blue light (caused by LACE) and without chromatophores expanded, using a custom build microrespirometry system (*SI Appendix*, Fig. S1). Oxygen consumption was measured during four alternating 5-min periods of chromatophore expansion and contraction (Fig. 1). We found a significant relationship between $\dot{V}O_2$ and oxygen concentration at which $\dot{V}O_2$ was measured (Fig. 2*A*, linear regression with ANOVA, $P = 0.016$). Therefore, we corrected oxygen consumption rates based on this relationship to an oxygen concentration of 240 µmol O_2 L^{-1}. The area-specific oxygen consumption rate of chromatophores was determined by taking the oxygen consumption rate mean difference of periods of chromatophore expansion and contraction divided by the difference in area of skin covered by chromatophores during the chromatophore expanded period and chromatophore contracted periods.

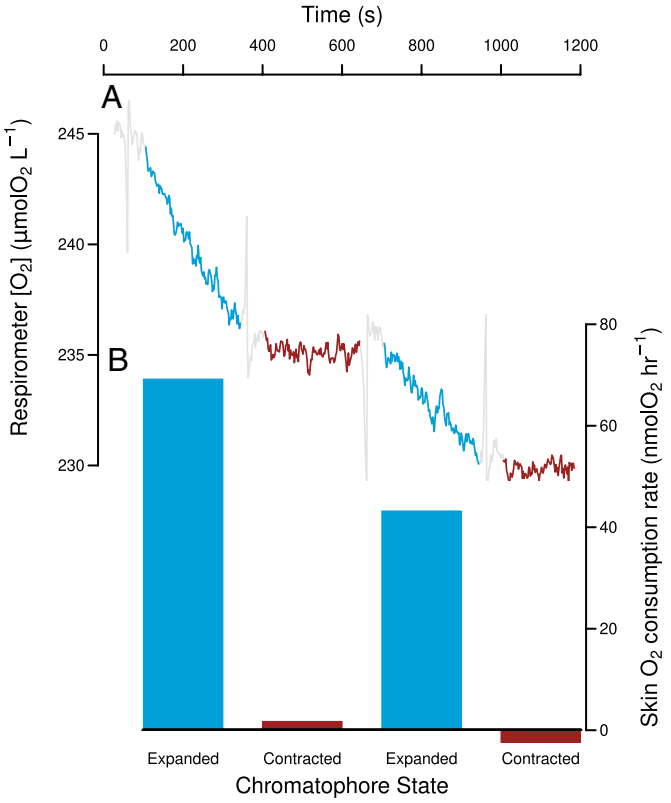

Fig. 1. Example oxygen consumption in octopus skin relative to chromatophore state over time. (*A*) Line plot of respirometer O_2 concentration over time, distinguished by two chromatophore states: expanded (blue) and contracted (red). Gray line indicates data excluded from analyses at transition between chromatophore states. (*B*) Skin oxygen consumption rate under expanded and contracted chromatophore states, corresponding to time periods directly above in panel (*A*).

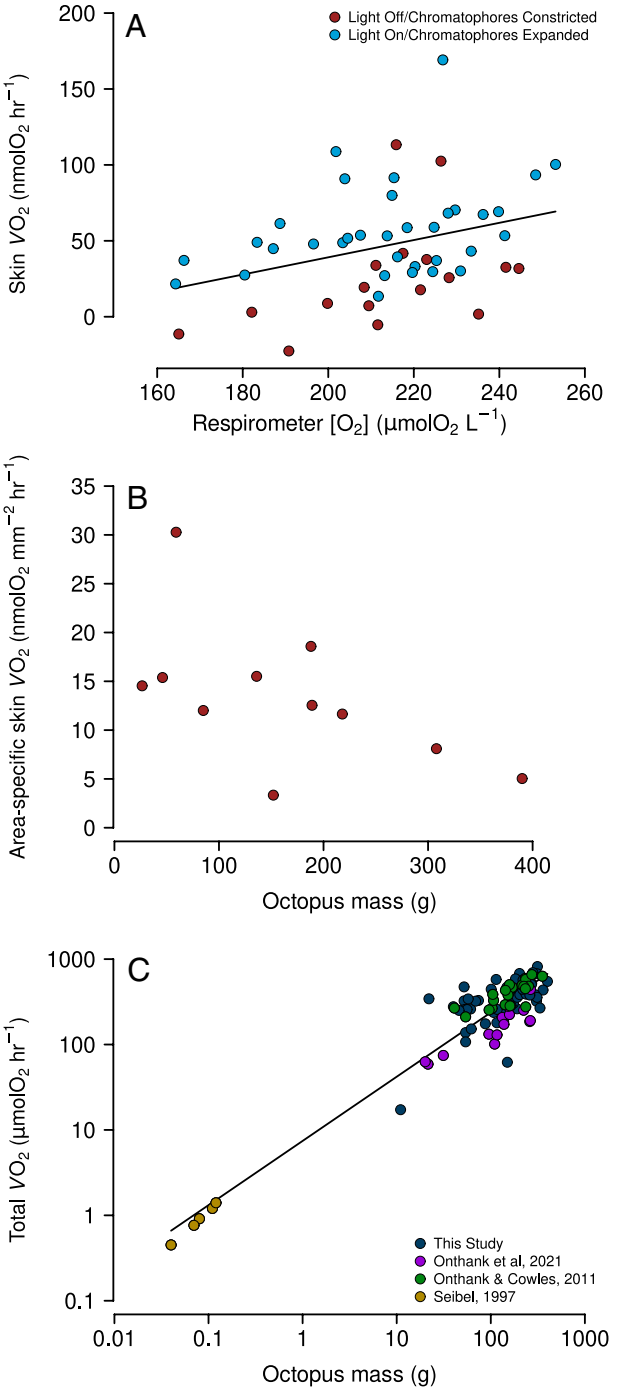

Fig. 2. Oxygen consumption patterns in *O. rubescens* relative to light conditions and body mass. (*A*) Oxygen consumption rate ($\dot{V}O_2$) as a function of ambient oxygen concentration, distinguished by light conditions and chromatophore activity. Relationship is significant (Linear regression, y = 0.5677 × −74.386, ANOVA, $P = 0.016$, $r^2 = 0.1127$). (*B*) Area-specific $\dot{V}O_2$ plotted against octopus body mass. Relationship is not significant (Linear regression, ANOVA, $P = 0.069$) (*C*) Total resting $\dot{V}O_2$ in relation to octopus mass, with data from multiple studies (nonlinear least squares regression, y = 7.433 × 0.751).

The chromatophore area-specific $\dot{V}O_2$ was significantly greater than 0 (one-sample *t* test, $P < 0.0001$) with a median value of 12.5 nmol O_2 mm^{-2} h^{-1} (95% CI 8.1 – 15.5 nmol O_2 per mm^2 per h). We found a nonsignificant relationship between *O. rubescens* mass of octopuses between 26 g and 390 g and skin area-specific $\dot{V}O_2$ (Fig. 2*B*, linear regression, ANOVA, $P = 0.069$) and therefore did not correct skin oxygen consumption based on octopus mass. However, the low *P*-value may indicate that more investigation of this relationship is warranted.

Modeling Octopus Oxygen Consumption Rates. In order to model the relationship between octopus mass and routine metabolic rate (RMR), resting oxygen consumption rates (VO_{2rest}) values were measured for octopuses in this study (*SI Appendix, Extended Methods*) and were obtained from published sources (11–13) for octopuses of masses from 0.04 g to 400 g. Virtually, all of these measurements were taken with the octopus kept in darkness to minimize disturbance to the octopus but would also minimize the use of the chromatophore system by the octopuses. Therefore, these VO_2 measurements involve minimal contribution of metabolic demand from the chromatophore system. From these data, we found the relationship to be

$$VO_{2rest} = 7.433\mathrm{m}^{0.751},$$

where VO_{2rest} is resting oxygen consumption rate (μmol O_2 h^{-1}), and m is octopus mass in grams (Table 1 and Fig. 2*C*).

Estimates of the surface area–mass relationship in *O. rubescens* were determined by using a Shining 3D Einscan-SP for octopuses that were 33 g and 377 g. The surface areas were 14,826 and 96,929 mm^2, respectively. The relationship between *O. rubescens* surface area and mass was:

$$\mathrm{S} = 1001\mathrm{m}^{0.77},$$

where S is surface area (mm^2) and m is mass (g). This relationship makes it possible to estimate the surface area based on a given mass of *O. rubescens* (Fig. 3*A*). Using this surface area–mass relationship and the area-specific chromatophore oxygen consumption rate, we were able to model the chromatophore oxygen consumption rate (VO_{2chrom}), the energy required for all chromatophores to be simultaneously active, for an octopus of a given mass (Fig. 3 *B* and *C*). Our data show that the energy allocated to chromatophore function is nearly as high as energy allocated to all other processes (RMR) when the octopus is at rest (Fig. 3*D*). For example, our estimated VO_{2rest} of a 100 g octopus would be 237 μmol O_2 h^{-1}, while our estimate for the VO_{2chrom} of a 100 g octopus would be nearly as high at 219 μmol O_2 h^{-1} (Table 1).

Table 1. Quantitative relationships and values for octopus skin oxygen consumption, whole octopus oxygen consumption rate, and area-mass parameters

Measurement	Value or Relationship
Skin oxyconformation relationship	VO_{2skin}=0.5677O_2−74.386
Whole octopus resting VO_2 vs. mass relationship	VO_{2rest}=7.433$m^{0.7517}$
Octopus area vs. mass relationship	A = 1001.1$m^{0.7709}$
Area-specific chromatophore system VO_2	12.54 nmol O_2 mm^{-2} h^{-1} (95% CI: 8.10-15.51)
Chromatophore VO_2 vs. mass relationship	$VO_{2rchrom}$ = 12.56$m^{0.7709}$
Estimated VO_{2rest} in a 100 g *O. rubescens*	237 μmol O_2 h^{-1}
Estimated $VO_{2rchrom}$ in a 100 g *O. rubescens*	219 μmol O_2 h^{-1}

VO_{2skin} is skin oxygen consumption in nmol O_2 mm^{-2} h^{-1}, A is area in mm^2, VO_{2rest} is resting oxygen consumption rate in μmol O_2 h^{-1}, m is mass is grams, and $VO_{2rchrom}$ is the oxygen consumption rate of the chromatophore system when fully activated in μmol O_2 h^{-1}.

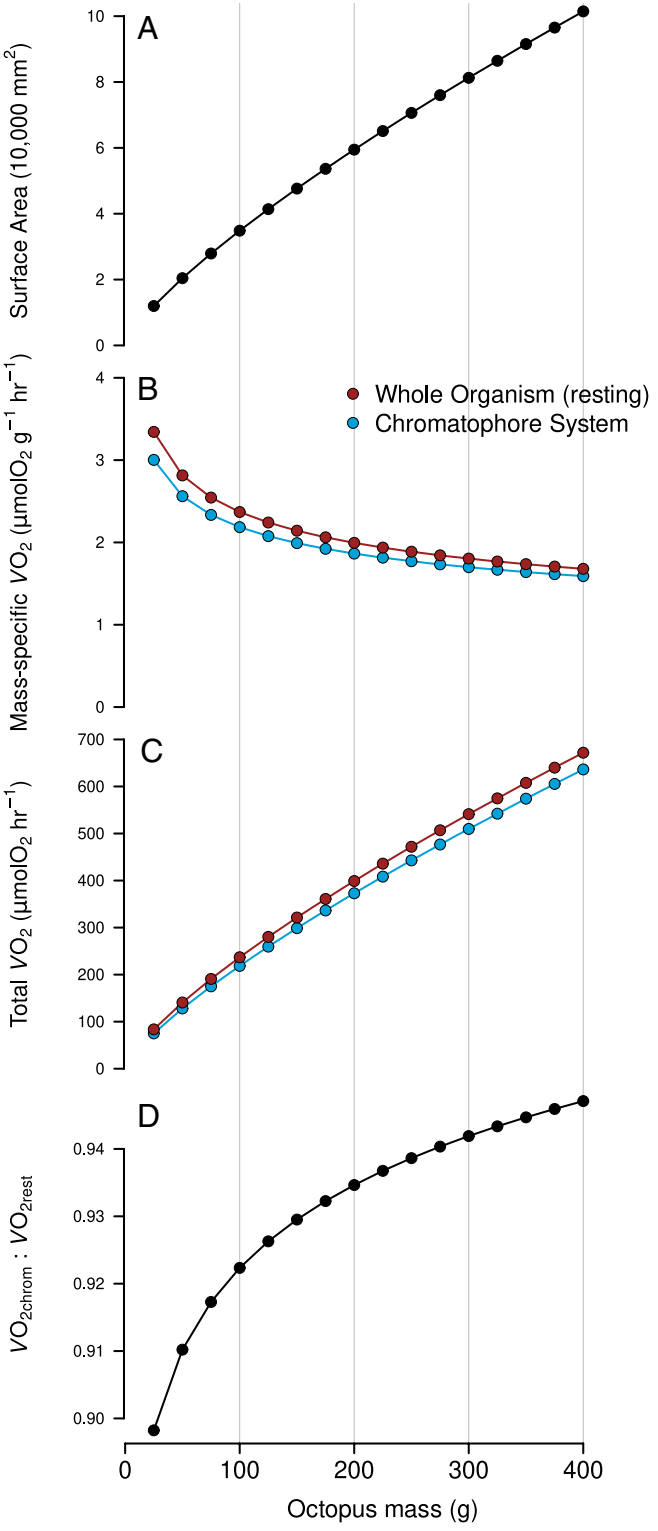

Fig. 3. (*A*) Surface area in relation to octopus mass, demonstrating an increase in surface area with octopus size. (*B*) Mass-specific oxygen consumption rate (VO_2) comparison between the whole organism (resting VO_2 rate performed in dark and therefore with minimal chromatophore system involvement) and the chromatophore system. (*C*) Total VO_2 changes with octopus mass for both whole organism and chromatophore system. (*D*) Ratio between chromatophore VO_2 and resting VO_2 as a function of octopus mass.

Discussion

The chromatophore system of coleoid cephalopods enables an exquisite form of dynamic camouflage and communication that is unparalleled in the animal kingdom. However, in this

investigation into the energy demand of the chromatophore system, we show that this unique system comes with a high cost. Our results show that the octopus chromatophore system has an exceptionally high metabolic demand; the complete activation of the chromatophore system requires nearly the same amount of energy as the rest of the organism when the octopus is at rest (RMR). Due to the involvement of the nervous and muscular systems, it is likely that cephalopod color change is one of the most energetically expensive forms of color change, so our estimate likely represents the upper bound of the cost of color change in the animal kingdom. While the chromatophore system, and the color change ability it confers, has long been understood to have a significant influence on the evolution of coleoid cephalopods, the dramatic cost to operate this system and the role that cost plays in the evolution of the chromatophore system has not yet been explored.

With this high metabolic cost of maintaining expanded chromatophores to support color change in octopuses, it would be expected that there would be strong selective pressure to develop physiological or behavioral methods to mitigate this energy cost (2). One such potential behavior method could be to adopt a nocturnal lifestyle, reducing the need for visual crypsis. While there is evidence that *O. rubescens*, the species used in this study, is not strongly nocturnal (14), many other octopus species are somewhat or strongly nocturnal (15–19). Another potential cost mitigation strategy could include the use of dens, which is a near-universal life history trait among shallow-water octopuses. Octopuses outside of dens employ high degrees of crypsis, and consequently, a high proportion of chromatophores are active, the majority of the time (20). However, octopuses in dens would be hidden from predators and not actively hunting prey, and therefore unlikely to be using their chromatophore system extensively. This reduction in energetic demand may be the reason that many octopus species spend the majority of their time in dens (14, 21).

Additionally, this high energetic cost of the chromatophore system would predict that this system would rapidly be lost when the risk of predation by visual predators or need to hunt for visual prey is lessened. This is exactly the pattern we see with the repeated, independent reduction of the chromatophore system in deep-sea octopus clades, such as those in the families Graneledonidae, Bathypolypodidae, and Enteroctopodidae (22).

Much work has been undertaken in the realm of octopus energetics, both in context of the surging interest in octopus aquaculture (23–25) and to explore the energetic trade-offs of octopus foraging (12, 26). While many of these studies do measure total metabolic rate of octopuses, none to date account for energy allocation to crypsis. This omission is particularly impactful in understanding the energetics of octopus foraging as octopuses spend the majority of hunting bouts heavily using their chromatophore system for camouflage (20). For instance, Mather and O'Dor when investigating foraging strategies of juvenile *Octopus vulgaris* found only 12% of daylight hours are spent foraging (26). Their explanation for this observation is that minimizing foraging time also minimizes risk of predation (26). While this explanation is likely correct, it is probably also incomplete as it does not account for the outlay of energy to the chromatophore system during foraging and the energetic savings incurred by reducing foraging time.

The persistence of the chromatophore system and the accompanying high metabolic demand evidences the great importance of this system in cephalopod survival strategies. While this system is exceptionally energetically expensive, it has aided cephalopods to become an exceptionally successful clade which are found in virtually all marine environments. The trade-offs between energy costs and the advantages of sophisticated camouflage undoubtedly have left their mark throughout cephalopod biology, many of which are certainly yet to be discovered.

Materials and Methods

Experimental Design. The purpose of this study was to determine the metabolic cost of chromatophore use of the ruby octopus (*O. rubescens*). Whole-organism oxygen consumption rate ($\dot{V}O_2$), a common proxy for metabolic rate, was measured using flow-through respirometry and comparable data was obtained from previously published studies. The strategy for isolating and measuring the metabolic rate of chromatophores was to use LACE to manipulate chromatophores on excised skin to expand and contract while in a small respirometer. Mass-specific $\dot{V}O_2$ measurements of the chromatophore system of a whole octopus were then compared to those of whole octopus resting $\dot{V}O_2$ measurements.

Octopus Collection and Housing. From June to August 2020, 12 male and 5 female *O. rubescens* ranging in size 26.5 g to 390 g were collected by SCUBA from Driftwood Beach, Whidbey Island, Washington (*SI Appendix*, Table S1). Octopuses were then transported to Rosario Beach Marine Laboratory (RBML) in Anacortes, WA, where the remainder of the work occurred. Once at RBML, each octopus was housed in an individual 27.3 L (30.8 cm × 24.5 cm × 36.2 cm) clear plastic tank with flowing seawater at approximately 13 °C and provided with a red-colored Nalgene water bottle as a den. Octopuses were kept with an approximately natural day:night cycle and fed one purple shore crab (*Hemigrapsus nudus*) each day.

Respirometry. A custom microrespirometry system composed of a 3D-printed PLA panel sandwiched between glass slides and sealed with silicone grease was developed to measure oxygen consumption rates in excised skin of *O. rubescens*. The system included a stir bar chamber with a 3D-printed stir bar, a DC motor attached to a neodymium magnet to drive the stir bar, channels to prevent bubble formation, and temperature control using a Peltier device. An Arduino Uno controlled light-emitting diodes (LEDs), stir bar speed, and temperature, and using proportional–integral–differential control ensured stable conditions. The build files necessary to produce this microrespirometer are available on the Zenodo repository at https://zenodo.org/doi/10.5281/zenodo.10182718 (27). Skin oxygen consumption rates were measured for 5 min under blue and red LED illumination, activating chromatophores, followed by a subsequent 5 min period with only red LEDs, deactivating chromatophores, with both cycles repeated. During each of these different lighted periods, photographs of the skin sample were taken under a dissecting microscope to verify chromatophore activation or inactivation. Using these photographs, the areas covered by chromatophores during each period were measured using ImageJ. See *SI Appendix, Extended Methods* on the construction of respirometry system, respirometry methods, and photograph analysis.

3D Scanning. Two octopuses preserved in formalin were used to determine the relationship between octopus surface area and wet mass (*SI Appendix*, Table S1). Wet masses of the octopuses were taken while alive. Octopuses were then placed into 2.5% ethanol in seawater to be sedated, then ethanol concentration was raised to 10% to kill the octopuses, which were then fixed in 12% formalin. Octopuses were 3D-scanned using a structured-light process with a Shining3D Einscan-SP desktop 3D scanner. To achieve a complete scan on the octopuses, the arms were removed from the body of the octopus and scanned separately.

All parts of both preserved octopuses were scanned using an EinScan desktop 3D scanner and each part was saved as a separate file. Surface area of 3D mesh files was calculated using MeshLab v2020.12 (28).

Oxygen Consumption Rate Data Analysis. Because the Pyroscience FirestingO2 and the Arduino data recording were not started exactly simultaneously, data collected from these devices were synchronized by using the peaks in oxygen and temperature measurements. Next, recorded oxygen measurements were corrected to 19 °C according to the measured relationship between temperature and oxygen using the empirically determined adjustment multiplier (*SI Appendix, Extended Methods*):

$$M = 3.22 \times 10^{-6} T^{3.68} + 0.834,$$

where M is the oxygen adjustment multiplier which would be multiplied by the measured oxygen to correct for temperature and T is the temperature in degrees Celsius.

In addition to correcting for temperature, the oxygen measurements were corrected to account for additional background light present when the blue LEDs were illuminated, which causes an apparent depression of the oxygen measurement. The background light correction was individually determined for each trial by selecting an oxygen measurement offset in which the beginning and end of the oxygen concentrations during each light period were aligned with that of the previous and subsequent light period.

From each 5-min period of light, 45 s were trimmed from the beginning and 15 s were trimmed from the end. This was due to unstable oxygen readings during the transitions between red and blue light periods and vice versa.

Oxygen consumption rate for each light period (5 min blue+red, 5 min red, 5 min blue+red, 4 min red) was calculated by finding the slope of a linear regression of oxygen measurements in $\mu mol\ L^{-1}$ vs. time in seconds during the time period in question, which gave oxygen consumption in $\mu mol\ O_2\ L^{-1}\ s^{-1}$. This number was multiplied by 3,600 to give $\mu mol\ O_2\ L^{-1}\ h^{-1}$ then multiplied by 0.000612L (the volume of the respirometer) to convert to $\mu mol\ O_2\ h^{-1}$ then multiplied by 1,000 to report oxygen consumption rate values in $nmol\ O_2\ h^{-1}$.

The oxygen consumption rate was corrected for the oxygen level of the respirometer when the measurement was taken as there was a statistically significant positive relationship between oxygen concentration in the respirometer and measured oxygen consumption rate (Fig. 2*A*). To do this, the relationship between oxygen consumption rates and oxygen levels was determined using a linear regression. Each oxygen consumption measurement was then corrected to a pO_2 of 240 $\mu mol\ O_2\ L^{-1}$ (Fig. 2*A*).

Two of the trials included a small bubble in the respirometer that required correction as well. The diameter of each bubble was measured using FIJI (FIJI Is Just ImageJ) by calibrating the measurement tool using the known measurement of the temperature probe within the respirometer. The volume of each bubble was estimated from its diameter assuming that it was a sphere. The "correct bubble" function in the R package "respirometry" was used to adjust to the realized volume of the respirometer (29).

After the bubble correction, the average oxygen consumption from the red-light period, when chromatophores were more contracted, was subtracted from that of the average of the two blue light periods, when chromatophores were more expanded. Data from three octopuses, 7, 14, and 15, in which the chromatophore area decreased during blue light periods were removed since they did not exhibit LACE (*SI Appendix*, Table S1). Finally, the change in oxygen consumption rate was divided by the change in chromatophore coverage area to arrive at the oxygen consumption per area chromatophore coverage in $nmol\ O_2\ mm^{-2}\ h^{-1}$.

Oxygen was measured at 19 °C since this was near room temperature. In trials, when the peltier was set to cool the water below room temperature, condensation formed on the respirometer. The condensation required periodic removal by being wiped off, which could slightly alter the position of the respirometer. For more accurate data and consistent positioning of the respirometer, it was maintained at room temperature for all trials. Thus, $\dot{V}O_2$ measurements were adjusted from 19 °C to 11 °C the temperature at which previous whole-organism $\dot{V}O_2$ was measured, assuming a Q_{10} of 2. Finally, Tukey's fences were used to identify and remove outlier oxygen consumption per area values (30). A *t* test was then performed to determine whether the increase in $\dot{V}O_2$ under blue light was greater than 0.

Calculating Chromatophore Metabolic Rate of Whole Octopus by Mass. The relationship between octopus mass and surface area was determined by using the previously described surface area data determined from 3D scans of preserved octopuses. The nls (nonlinear least squares) function in R was used to fit an equation to the data in the form of $A = aM^b$, where A is surface area, M is mass of the octopus, and a and b are the scaling coefficient and power to be determined by the fitting process. For octopuses of masses between 25 g and 400 g, we then modeled $\dot{V}O_2$ due to chromatophore activation in an octopus of a given mass by using this relationship to determine the surface area based on mass, then multiplied the surface area by our mean chromatophore oxygen consumption per unit area. This result was divided in half because chromatophore density is higher on the dorsal surface of the octopuses than the ventral surface. This likely underestimates the chromatophore density on the octopus and, therefore, gives a conservative estimate of metabolic cost of the chromatophore system.

Determination of Whole Organism Resting $\dot{V}O_2$. Whole organism resting $\dot{V}O_2$ for *O. rubescens* were determined using flow-through respirometry in June through August in the summers of 2015 and 2017 following closely published procedures (12, 13). In brief, octopuses were placed into a size-matched respirometer (volume 100 to 1,000 mL). Each respirometer was filled with seawater that had been passed through a 5 micron filter and ultraviolet light sterilized. A Masterflex L/S variable speed peristaltic pump was used to flow seawater through the respirometry system at no less than $10\ mL\ min^{-1}$, and flow rates were verified at the beginning and end of each respirometry measurement by measuring the time required for the system outflow to fill a 100 mL graduated cylinder, and flow was also continuously measured during respirometry with a uxcell 0.1 to 4.5 L min^{-1} electronic water flow count sensor. PyroScience Firesting O2 flow-through cells (OXFTC2) and robust temperature probes (TSUB36) were placed on the incurrent and excurrent stream of each respirometer. RMR was measured for each octopus over a 23-h period and the first 3 h of each measurement were discarded to account for acclimation of the octopus to the respirometer. During respirometry, a black cloth was placed over the clear acrylic top of the respirometer to keep the octopus calm. RMR was calculated from oxygen concentration and flow rate data using the "OTools" package (31) in R (32). Additional RMR measurements of *O. rubescens* were taken from literature sources (11–13).

Chromatophore $\dot{V}O_2$ Comparison to Whole Octopus Resting $\dot{V}O_2$. Resting $\dot{V}O_2$ data previously measured in 97 *O. rubescens* as described above were used for comparison to chromatophore system $\dot{V}O_2$ estimates. Most of these data were collected at 11 °C but that which was not was corrected to a temperature of 11 °C based on a Q_{10} of 2. The scaling exponent among these previous measurements was determined using a linear regression of the log–log transformed data. This scaling exponent was then used in conjunction with the nls() function to determine the relationship between $\dot{V}O_2$ and octopus mass (Fig. 2*C*).

Data, Materials, and Software Availability. All data and code supporting these analyses are available at the following Zenodo repository: https://zenodo.org/doi/10.5281/zenodo.10182790 (33) and https://zenodo.org/doi/10.5281/zenodo.10182718 (27).

ACKNOWLEDGMENTS. Our colleague, Dr. Lloyd Trueblood, assisted us in conceptualizing the research question and has reviewed the manuscript prior to its submission. Additionally, we were assisted by D. Cowles, C.J. Brothers, J. Nestler, A. Verde, and J. D'Auria by helping collect the octopuses used in the study and J. Sereewit by assisting in husbandry and data collection.

1. D. Stuart-Fox, A. Moussalli, Camouflage, communication and thermoregulation: Lessons from colour changing organisms. *Philos. Trans. R. Soc. Lond. B Biol. Sci.* **364**, 463–470 (2009).
2. A. Alfakih, P. J. Watt, N. J. Nadeau, The physiological cost of colour change: Evidence, implications and mitigations. *J. Exp. Biol.* **225**, jeb210401 (2022).
3. R. C. Duarte, A. A. Flores, M. Stevens, Camouflage through colour change: Mechanisms, adaptive value and ecological significance. *Philos. Trans. R. Soc. B Biol. Sci.* **372**, 20160342 (2017).
4. G. M. Rodgers, N. W. Gladman, H. F. Corless, L. J. Morrell, Costs of colour change in fish: Food intake and behavioural decisions. *J. Exp. Biol.* **216**, 2760–2767 (2013).
5. N. Polo-Cavia, I. Gomez-Mestre, Pigmentation plasticity enhances crypsis in larval newts: Associated metabolic cost and background choice behaviour. *Sci. Rep.* **7**, 39739 (2017).
6. R. T. Hanlon *et al.*, "Rapid adaptive camouflage in cephalopods" in *Animal Camouflage: Mechanisms and Functions*, M. Stevens, S. Merilaita, Eds. (Cambridge University Press, 2011), pp. 145–163.
7. J. B. Messenger, Cephalopod chromatophores: Neurobiology and natural history. *Biol. Rev. Camb. Philos. Soc.* **76**, 473–528 (2001).
8. A. Packard, G. D. Sanders, Body patterns of *Octopus vulgaris* and maturation of the response to disturbance. *Anim. Behav.* **19**, 780–790 (1971).
9. R. T. Hanlon, The functional organization of chromatophores and iridescent cells in the body patterning of *Loligo plei* (Cephalopoda: Myopsida). *Malacologia* **23**, 89–119 (1982).
10. M. D. Ramirez, T. H. Oakley, Eye-independent, light-activated chromatophore expansion (LACE) and expression of phototransduction genes in the skin of *Octopus bimaculoides*. *J. Exp. Biol.* **218**, 1513–1520 (2015).
11. B. A. Seibel, E. V. Thuesen, J. J. Childress, L. A. Gorodezky, Decline in pelagic cephalopod metabolism with habitat depth reflects differences in locomotory efficiency. *Biol. Bull.* **192**, 262–278 (1997).
12. K. L. Onthank, D. L. Cowles, Prey selection in *Octopus rubescens*: Possible roles of energy budgeting and prey nutritional composition. *Mar. Biol.* **158**, 2795–2804 (2011).
13. K. L. Onthank, L. A. Trueblood, T. Schrock-Duff, L. G. Kore, Impact of short- and long-term exposure to elevated seawater Pco_2 on metabolic rate and hypoxia tolerance in *Octopus rubescens*. *Physiol. Biochem. Zool.* **94**, 1–11 (2021).
14. J. W. Humbert, K. Williams, K. L. Onthank, Den-associated behavior of *Octopus rubescens* revealed by a motion-activated camera trap system. *Integrat. Comp. Biol.* **62**, 1131–1143 (2022).
15. D. L. Sinn, Patterns of activity cycles in juvenile California two-spot octopuses (*Octopus bimaculoides*). *Am. Malacol. Bull.* **24**, 65–69 (2008).

16. D. V. Meisel, R. A. Byrne, M. Kuba, U. Griebel, J. A. Mather, "Circadian rhythms in Octopus vulgaris" in *Coleoid Cephalopods through Time*, S. V. Warnke, K. Keupp, H. Boletzky, Eds. (Berline, 2003), pp. 171–177.
17. C. S. Cobb, S. K. Pope, R. Williamson, Circadian rhythms to light-dark cycles in the lesser octopus, *Eledone cirrhosa*. *Mar. Freshwater Behav. Physiol.* **26**, 47–57 (1995).
18. E. R. Brown, S. Piscopo, R. De Stefano, A. Giuditta, Brain and behavioural evidence for rest-activity cycles in *Octopus vulgaris*. *Behav. Brain Res.* **172**, 355–359 (2006).
19. D. Scheel, L. Bisson, Movement patterns of giant Pacific octopuses, *Enteroctopus dofleini* (Wülker, 1910). *J. Exp. Mar. Biol. Ecol.* **416–417**, 21–31 (2012).
20. R. T. Hanlon, J. W. Forsythe, D. E. Joneschild, Crypsis, conspicuousness, mimicry and polyphenism as antipredator defences of foraging octopuses on Indo-Pacific coral reefs, with a method of quantifying crypsis from video tapes. *Biol. J. Linnean Soc.* **66**, 1–22 (1999).
21. C. E. O'Brien, *et al.*, Octospy: What *Octopus insularis* do in their dens. *Mar. Ecol.* **44**, e12763 (2023), 10.1111/maec.12763.
22. J. R. Voight, Observations of deep-sea octopodid behavior from undersea vehicles. *Am. Malacol. Bull.* **24**, 43–50 (2008).
23. M. Nande, J. Iglesias, P. Domingues, M. Pérez, Effect of temperature on energetic demands during the last stages of embryonic development and early life of *Octopus vulgaris* (Cuvier, 1797) paralarvae. *Aquaculture Res.* **48**, 1951–1961 (2017).
24. C. Rosas *et al.*, Energy balance of *Octopus maya* fed crab or an artificial diet. *Mar. Biol.* **152**, 371–381 (2007).
25. C. Rosas *et al.*, Effect of type of binder on growth, digestibility, and energetic balance of *Octopus maya*. *Aquaculture* **275**, 291–297 (2008).
26. J. A. Mather, R. K. O'Dor, Foraging strategies and predation risk shape the natural history of juvenile *Octopus vulgaris*. *Bull. Mar. Sci.* **49**, 256–269 (1991).
27. K. L. Onthank, Microrespirometer. Zenodo. https://doi.org/10.5281/zenodo.10182718. Deposited 21 November 2023.
28. P. Cignoni *et al.*, "Meshlab: An open-source mesh processing tool" in *Eurographics Italian Chapter Conference*, V. Scarano, R. De Chiara, U. Erra, Eds. (The Eurographics Association, 2008), pp. 129–136.
29. M. A. Birk, respirometry: Tools for conducting and analyzing respirometry experiments. Comprehensive R Archive Network. https://cran.r-project.org/package=respirometry. Deposited 7 July 2023.
30. J. W. Tukey, *Exploratory Data Analysis* (Addison-Wesley, 1977).
31. K. L. Onthank, OTools. Github. https://github.com/KirtOnthank/OTools. Deposited 6 June 2023.
32. R Development Core Team, *R: A Language and Environment for Statistical Computing* (R Foundation for Statistical Computing, 2008).
33. K. L. Onthank, Octopus chromatophore metabolism. Zenodo. https://doi.org/10.5281/zenodo.10182790. Deposited 30 September 2024.